

# Ammonia Borane as a Hydrogen Carrier: Dehydrogenation and Regeneration

Nathan C. Smythe<sup>[a]</sup> and John C. Gordon<sup>\*[a]</sup>

**Keywords:** Hydrogen storage / Dehydrogenation / Homogeneous catalysis / Transition metals / Ammonia borane

Interest in sustainable non-hydrocarbon-based fuels for transportation has grown as the realization that the supply of fossil fuels is limited and the deleterious environmental effects of burning them has come into public focus. The use of hydrogen ( $H_2$ ) has been proposed as an alternative, but its use in pure form is undesirable due to the high pressures or low temperatures required to store useful quantities. Approaches to ameliorate this issue, which stem from the low volumetric energy density of  $H_2$ , include the pursuit of sorbents capable of containing  $H_2$  in greater density than liquid  $H_2$  at reasonable temperatures and pressures, metal hydrides such as  $NaBH_4$ , and chemical hydrides such as ammonia bo-

rane (AB,  $NH_3BH_3$ ). AB contains 19.6 wt.-%  $H_2$ , which is well suited to practical applications, but issues with extracting the optimal quantities of  $H_2$  at reasonable temperatures and at useful rates as well as recycling of the spent fuel back into AB with good efficiency and reasonable cost remain to be solved. These problems are inextricably intertwined, as the needs of the regeneration process dictate which catalysts are used (i.e. what kind of spent fuel is generated). This Microreview focuses on recent developments in transition metal complexes for the catalytic dehydrogenation of AB. *Neither solvolysis of AB nor thermolysis of AB in the absence of a catalyst are covered in this review.*

## 1. Introduction

Within the last several years there has been increasing interest in the use of hydrogen ( $H_2$ ) as a transportation fuel. One of the reasons for this is the fact that  $H_2$  has a high energy content per mass unit ( $120 \text{ MJ kg}^{-1}$ ) vs. that of petroleum ( $44 \text{ MJ kg}^{-1}$ ). Another benefit of  $H_2$  is that it can be used to run a fuel cell which increases efficiencies compared to an internal combustion engine, simultaneously eliminating the formation of sulfur and nitrogen oxide emis-

sions as well as carbon particulates that are detrimental to the environment. On the down side,  $H_2$  has a low energy content per unit volume [ $0.01 \text{ kJ L}^{-1}$  at STP ( $8.4 \text{ MJ L}^{-1}$  for liquid  $H_2$ ) vs.  $32 \text{ MJ L}^{-1}$  for petroleum]. For transportation applications, a fuel should ideally possess a high energy content in a small volume (to accommodate passengers on-board) as well as the minimum weight possible in order to maintain overall fuel efficiency.<sup>[1,2]</sup>

As has been noted elsewhere,<sup>[2,3]</sup> the U.S. Department of Energy (DOE) has established a series of volume and weight capacities in order that a vehicle can travel > 300 miles on a single fill. These recently updated targets include gravimetric [4.5 wt.-% (2010), 5.5 wt.-% (2015), and 7.5 wt.-% (ultimate)] and volumetric [ $3.2 \text{ MJ L}^{-1}$  (2010),  $4.7 \text{ MJ L}^{-1}$  (2015), and  $8.3 \text{ MJ L}^{-1}$  (ultimate)] capacities that refer to

[a] Chemistry Division, MS J582,  
Los Alamos National Laboratory,  
Los Alamos, NM 87545, USA  
Fax: +1-505-667-9905  
E-mail: jgordon@lanl.gov



Nathan C. Smythe grew up in Culver City, California, USA. He received his B.Sc. from the University of California at Berkeley in 2001 where he worked under Prof. Jeffrey R. Long. He then joined Prof. Richard R. Schrock's group at MIT as a graduate student to work on dinitrogen reduction. After receiving his Ph.D. in 2006, he began a post-doctoral position at San Diego State University with Prof. Laurance Beauvais. In 2009 he began his current post-doctoral position at Los Alamos National Laboratory where he is currently working on catalysts for ammonia borane dehydrogenation.



John C. Gordon was born in Kilmarnock, Scotland in 1963. He received his B.Sc. (Hons) degree from the University of Glasgow in 1985 and his Ph.D. in Chemistry in 1990 from the University of Notre Dame. Dr. Gordon held postdoctoral positions at the University of Maryland (College Park) and at Los Alamos National Laboratory (LANL). After spending a brief period in the private sector, he returned to LANL as a Technical Staff Member. Between 2006 and 2008, John was Group Leader of the Inorganic, Isotope and Actinide Chemistry Group (C-IIAC) within Chemistry Division at LANL. Dr. Gordon's research interests broadly span the inorganic and organometallic chemistry of the 4f- and 5f-block elements, catalysis for energy efficient applications, biomimetic hydrogen production, and chemical hydrogen storage chemistries.

overall system requirements, i.e. this means that the  $H_2$  storage capacity is evaluated with respect to all associated components (valves, regulators, tank, piping, insulation, etc.).

Currently, there are four leading methodologies to store  $H_2$ : physical means (high pressure tanks), sorbents (nanoporous materials), metal hydrides, and so-called chemical hydrides. As these approaches have been described in several other excellent reviews,<sup>[4–12]</sup> this particular Microreview will focus on recent reports (particularly within the 2008–2009 timeframe) regarding the release of  $H_2$  from a specific chemical hydride (ammonia borane), using metal-based catalysts. *Therefore, neither solvolysis of AB nor thermolysis of AB in the absence of a catalyst are covered in this review.* Recent efforts toward the regeneration of dehydrogenated spent fuel materials will also be addressed.

### 1.1. Ammonia Borane (AB, $H_3NBH_3$ )

Chemical hydrides are typically composed of lighter elements than metal hydrides, resulting in higher gravimetric storage capacities in the former class. One of these molecules in particular, ammonia borane (AB,  $H_3NBH_3$ ), has received increasing attention by the scientific community with respect to its potential utility as a  $H_2$  storage material.<sup>[5]</sup> This molecule is stable in the solid state at ambient temperatures and has an impressive gravimetric capacity of 19.6 wt.-%  $H_2$  (6.5 wt.-% and 13.1 wt.-% for the first and second equivalents of  $H_2$ , respectively), potentially capable of meeting the DOE targets outlined above. While there have been several reports of AB dehydrogenation in the solid state and in solution, thermolysis occurs at temperatures that are too high (around 110, 150, and 1400 °C for the first, second, and third equivalents of  $H_2$ <sup>[11]</sup>) and at rates that are too slow while hydrolysis results in strong B–O

bonds that make regeneration difficult. Several groups have described the fact that metal complexes are also capable of catalyzing  $H_2$  loss from AB, and these kinds of metal-catalyzed methods offer the potential for greater extents of release at lower temperatures than thermal methodologies. It is clear however that more work needs to be done in order to understand the mechanism(s) by which these catalysts operate in order to optimize both the rate and extent of  $H_2$  release for practical usage of AB in a vehicular application.

Figure 1 details the abbreviations and structures of the dehydrogenation products of AB that will be used within the context of this Microreview. Removing one equivalent of  $H_2$  from AB yields aminoborane ( $NH_2BH_2$ ) which is an analogue of ethylene<sup>[13]</sup> that is highly reactive, and is only isolable at low temperatures.<sup>[14,15]</sup> Aminoborane readily oligomerizes to form products of the type  $(NH_2BH_2)_n$ . CTB [cyclotriborazane,  $(NH_2BH_2)_3$ ] is an analogue of cyclohexane that is a crystalline solid that is stable below 100 °C. Pentamer [cyclopentaborazane,  $(NH_2BH_2)_5$ ] has been characterized by IR spectroscopy, powder X-ray diffraction, and solution molecular weight experiments. The nature of PAB (polyaminoborane) is more nebulous as there are a variety of routes by which polymerization may occur, and as a result there are likely structures that are linear, branched, and cyclic.<sup>[5]</sup>

Iminoborane (NHBH) is an analogue of acetylene, and is the result of removing two equivalents of  $H_2$  from AB. Like aminoborane, it is only observable at low temperatures as it readily oligomerizes as temperature and concentration increase. Borazine,  $(NHBH)_3$ , is a well-defined iminoborane oligomer. Both PIB (polyiminoborane) and PB (polyborazylene, cyclic polyiminoborane) have ill-defined amounts of cross-linking and branching that are likely dependent on the synthetic conditions employed.

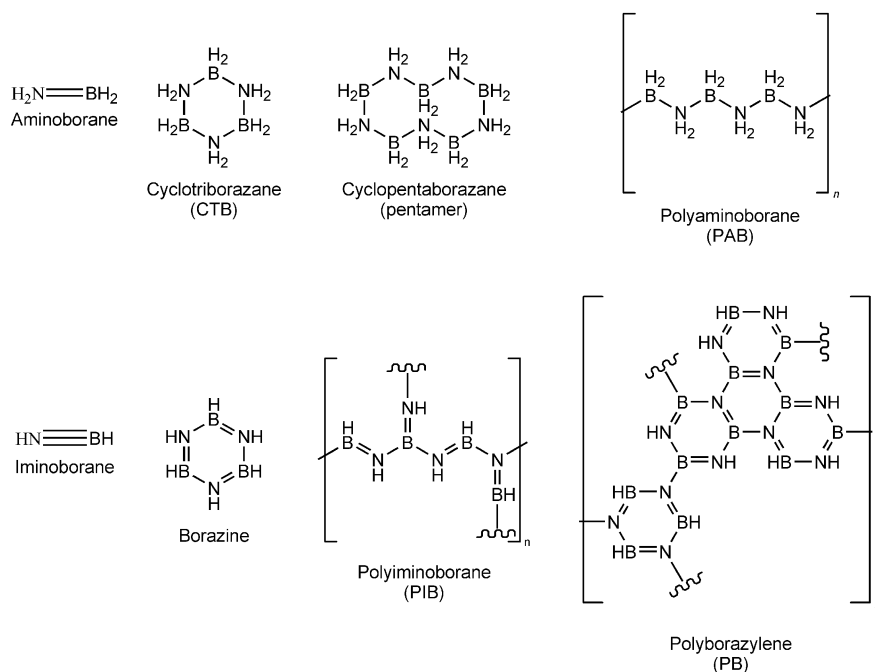


Figure 1. AB dehydrogenation products.<sup>[11]</sup>

## 2. Metal-Catalyzed Dehydrogenation

### 2.1. Retrospective

The first examples of metal-catalyzed amine-borane dehydrogenations were reported in 1989 using  $\text{Ru}_3(\text{CO})_{12}$ ,<sup>[16]</sup> and  $\text{Pd/C}$ .<sup>[17]</sup> In 2001, Manners et al. reported that  $[\text{Rh}(\text{1,5-COD})(\mu\text{-Cl})_2]$  (COD = cyclooctadiene) catalyzed the dehydrogenation of a number of amine boranes at room temperature or with mild thermolysis.<sup>[18]</sup> In 2003, the dehydrocoupling chemistry was extended to AB, whereupon the Manners group demonstrated that the catalyst precursor  $[\text{Rh}(\text{1,5-COD})(\mu\text{-Cl})_2]$  (328 K, in diglyme or tetraglyme) could dehydrogenate AB to form borazine along with other nonvolatile B–N-containing species via the cyclic trimer  $(\text{H}_2\text{NBH}_2)_3$  and  $\mu$ -aminoborane intermediates  $[(\mu\text{-NH}_2)\text{-B}_2\text{H}_5]$ .<sup>[19]</sup> Utilizing TEM, in the case of  $\text{MeH}_2\text{NBH}_3$ , catalyst poisoning experiments with mercury suggested that catalysis was in fact being promoted by heterogeneous rhodium clusters on the order of 2 nm in size. However, in situ monitoring of the reaction by XAFS and  $^{11}\text{B}$  NMR reported in 2005 suggests that a soluble  $\text{Rh}_6$  aggregate may be involved.<sup>[20]</sup> This was followed up by a more comprehensive study of the XAFS spectra in 2007<sup>[21]</sup> which corroborated this initial finding, identifying greater than 99% of the rhodium as  $\text{Rh}_{4-6}$  clusters with no indication of metallic rhodium when air is excluded.

Goldberg et al. reported the first example of homogeneous AB dehydrogenation by a well-defined catalyst in 2006.<sup>[22]</sup> Based on the isoelectronic nature of AB and ethane, the alkane dehydrogenation catalyst  $(\text{POCOP})\text{IrH}_2$ ,<sup>[23]</sup> [ $\text{POCOP} = \eta^3\text{-1,3-(OPtBu}_2)_2\text{C}_6\text{H}_3$ , Figure 2] was investigated, resulting in one equivalent of  $\text{H}_2$  loss per molecule of AB and quantitative formation of pentamer. This reaction occurs at room temperature and is complete in under 20 minutes when 1.0 or 0.5 mol-% of catalyst are used. Immediately upon addition of AB, the parent dihydride is converted into a reactive tetrahydride species, which is believed to be subsequently deactivated by coordination of  $\text{BH}_3$ . Addition of  $\text{BH}_3\cdot\text{THF}$  to the dihydride precursor results in an adduct that is unreactive towards AB. The tetrahydride complex can be restored under 30 psi  $\text{H}_2$ . More recent theoretical calculations on the mechanism suggest that despite the isoelectronic relationship between AB and ethane, the polar B–N bond induces an alternate mechanistic pathway.<sup>[24]</sup> Rather than the C–H oxidative addition pathway invoked in alkane dehydrogenation, the dehydrogenation of AB by  $(\text{POCOP})\text{IrH}_2$  proceeds through concerted removal of hydrogen.

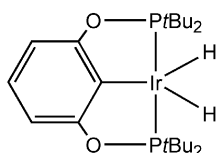
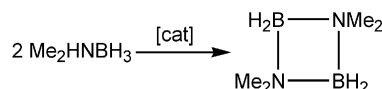


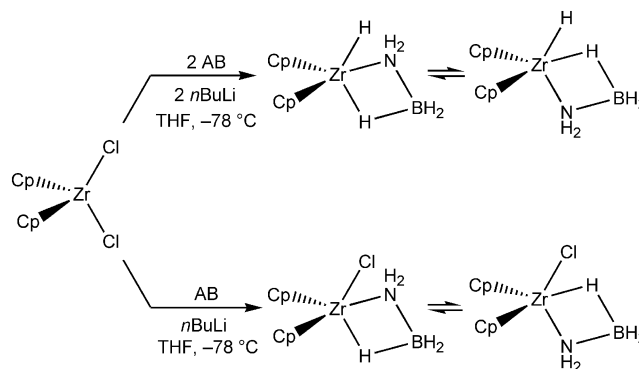
Figure 2.  $(\text{POCOP})\text{IrH}_2$ .

In 2006 and 2007, Manners et al.<sup>[25]</sup> and Chirik et al.<sup>[26]</sup> detailed titanium and zirconium metallocene catalysts capable of dehydrogenating  $\text{Me}_2\text{HNBH}_3$  to the cyclic dimer

$(\text{Me}_2\text{NBH}_2)_2$  (Scheme 1). While neither report explored the reaction of these metal complexes with AB, Roesler et al. did report on the reaction of AB with zirconocenes; albeit via  $\text{LiNH}_2\text{BH}_3$ .<sup>[27]</sup> The results are zirconium heterocycles containing the  $[\text{NH}_2\text{BH}_3]^-$  fragment with Zr–N and B–H–Zr bonds (Scheme 2) as determined by NMR spectroscopy and X-ray crystallography.



Scheme 1. Dehydrogenation of  $\text{Me}_2\text{HNBH}_3$  by titanium and zirconium metallocene catalysts.<sup>[25,26]</sup>



Scheme 2. Reactions of  $\text{Cp}_2\text{ZrCl}_2$  with AB.<sup>[27]</sup>

In 2007, Baker et al.<sup>[28]</sup> reported the most effective (in terms of extent of AB dehydrogenation) catalyst to date in the form of an N-heterocyclic carbene (NHC) supported nickel complex [NHC is the Enders' carbene (1,3,4-triphenyl-4,5-dihydro-1*H*-1,2,4-triazol-5-ylidene)].<sup>[29]</sup> The impetus for the choice of carbenes as supporting ligands was the observation of the decomposition of phosphane-supported iron and nickel complexes to black precipitate upon reaction with AB. At 60 °C in diglyme,  $\text{Ni}(\text{NHC})_2$  produced more than 2.5 equivalents of  $\text{H}_2$  (18 wt.-%) within hours (Scheme 6).  $^{11}\text{B}$  NMR spectroscopy of the dehydrogenation product revealed cross-linked borazine (PB). Measurements of the kinetic isotope effects (KIE) of deuterated AB analogues demonstrated that both N–H and B–H bonds are broken in the rate-determining step(s), but the mechanism was not completely elucidated. This still remains an area of active study (vide infra).

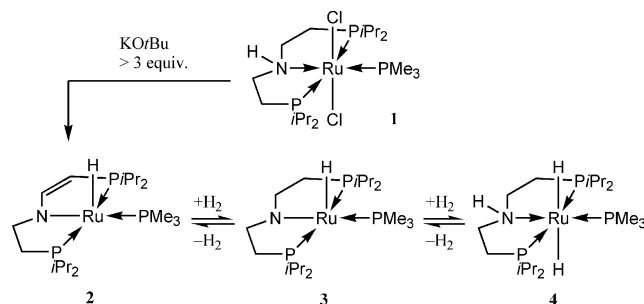
### 2.2. New Catalyst Developments

Along with their work on  $[\text{Rh}(\text{1,5-COD})(\mu\text{-Cl})_2]$ , Manners et al. also reported the dehydrogenation of  $\text{Me}_2\text{NH}\cdot\text{BH}_3$  (DMAB) using Wilkinson's catalyst,  $\text{RhCl}(\text{PPh}_3)_3$ . However, this reaction was slow, requiring 44 h to go to completion. More recently, this group has reported on the dehydrogenation chemistry of rhodium and iridium analogues of Wilkinson's catalyst supported by the secondary phosphane  $\text{PHCy}_2$  (Cy = cyclohexyl).<sup>[30]</sup> While these complexes are not new,<sup>[31]</sup> their reactivity towards

amine boranes had not previously been studied. Neither complex was effective in dehydrogenating AB, but various substituted amine boranes such as  $\text{Me}_2\text{NH}\cdot\text{BH}_3$ ,  $i\text{Pr}_2\text{NH}\cdot\text{BH}_3$ ,  $\text{MeBzNH}\cdot\text{BH}_3$  (Bz = Benzyl), and  $\text{MeNH}_2\cdot\text{BH}_3$  underwent varying degrees of hydrogen loss. The addition of  $\text{B}(\text{C}_6\text{F}_5)_3$  as a co-catalyst universally improved substrate consumption (except in the case of  $\text{MeNH}_2\cdot\text{BH}_3$  and rhodium, as rhodium already exhibits 100% conversion), including the reaction with AB (although in this case there was still minimal conversion for both rhodium and iridium). This enhancement in reactivity, along with the detection of  $\text{PHCY}_2\cdot\text{B}(\text{C}_6\text{F}_5)_3$  by NMR spectroscopy after the addition of one equivalent of  $\text{B}(\text{C}_6\text{F}_5)_3$ , supports the hypothesis that the active catalytic species is a diphosphane metal complex, although it was not detected in situ. Further support for the molecular rather than colloidal nature of catalysis was provided in the form of nano-filtration and mercury poisoning experiments along with kinetic measurements. Formation of black material (colloidal rhodium) was not observed, and filtration did not affect the color of the reaction. The efficacy of the reaction was not affected by filtration or the addition of mercury. Finally, the induction period that has been attributed to the formation of the active rhodium complex(es) from  $[\text{Rh}(\text{1,5-COD})\mu\text{-Cl}]_2$  was not observed in kinetic experiments.

Schneider and co-workers introduced a PNP-supported ruthenium complex (Scheme 3) for the dehydrogenation of AB<sup>[32]</sup> under the hypothesis that a bifunctional catalyst employing a Noyori-type mechanism<sup>[33–35]</sup> would be effective at this transformation due to the polar nature of the B–N bond. They approached this using *trans*- $[\text{RuCl}_2(\text{PMe}_3)(\text{PNP})]$  (**1**), to which was added  $\text{K}^+\text{O}^-\text{Bu}$  to yield enamido complex **2**. Under  $\text{H}_2$  (1 bar), **2** adds two equivalents of  $\text{H}_2$  to form amino complex **4** which then loses one equivalent of  $\text{H}_2$  under dynamic vacuum to form amido complex **3**. This reaction sequence was found to be further reversible, **3** reverting back to **2**, via loss of a second equivalent of  $\text{H}_2$  when left under argon for several days. While single crystals of **2** and **3** were not obtained, energy-minimized Density Functional Theory (DFT) models suggest that the coordination geometries of the enamido and amido complexes (**2** and **3** respectively) differ in that the former is best described as square pyramidal while the latter as a distorted trigonal bipyramid.

Using **3** in loadings between 0.01 and 0.1 mol-% in THF at room temperature, the dehydrogenation of AB was followed by measurement of evolved gas, giving from 0.83 to slightly over 1 equivalent of  $\text{H}_2$  (assuming  $\text{H}_2$  as the only gaseous product). However, the composition of the gas was not probed, and detection of borazine in the reaction mixture indicates that there is likely some contribution from species other than  $\text{H}_2$  to the measured gas volumes. The result of dehydrogenation was a white powder identified as  $[\text{H}_2\text{B-NH}_2]_n$  by MAS- $^{11}\text{B}$  NMR and IR spectroscopy. Measurements of kinetic isotope effects showed a significant difference between  $\text{H}_3\text{N-BH}_3$ ,  $\text{H}_3\text{N-BD}_3$  (2.1),  $\text{D}_3\text{N-BH}_3$  (5.2), and  $\text{D}_3\text{N-BD}_3$  (8.1), which is consistent with the concerted addition of AB. Addition of mercury to the reaction



Scheme 3. Synthesis and hydrogenation/dehydrogenation equilibria of PNP-supported ruthenium.<sup>[32]</sup>

mixture affected neither the kinetics nor the gaseous yield, indicating the observed reactivity occurs homogeneously in solution rather than heterogeneously at a reduced ruthenium colloid.

Recent work performed by Fagnou et al. focused on known and commercially available catalysts for the oxidation/reduction of alcohols (Figure 3).<sup>[36]</sup> The authors noted that while AB is isoelectronic with ethane, computational results<sup>[24,37]</sup> do not bear out this comparison in terms of reactivity, and that AB would be better compared to methanol in this regard. Further support for this comparison is the observation by Schneider that their ruthenium PNP complex demonstrated activity for the dehydrogenation of alcohols. Activating complexes **5–10** with 30 equivalents of  $\text{KO}^-\text{tBu}$  in THF led to the generation of up to one equivalent of  $\text{H}_2$  and the formation of an insoluble white material that was identified as polymeric aminoborane by comparison to previous reports.<sup>[22,38]</sup> The precatalysts leading to the most effective activity were the isopropyl and *tert*-butyl variants **5** and **6**, which generate one equivalent of  $\text{H}_2$  at 20 °C. It was also found that **5** produced two equivalents of  $\text{H}_2$  from  $\text{MeNH}_2\text{BH}_3$  under similar conditions. Consistent with the work reported by Schneider, dehydrogenation appears to occur through the concerted addition of AB as evidenced by DFT calculations on a model bis(amino-phosphane)Ru complex.

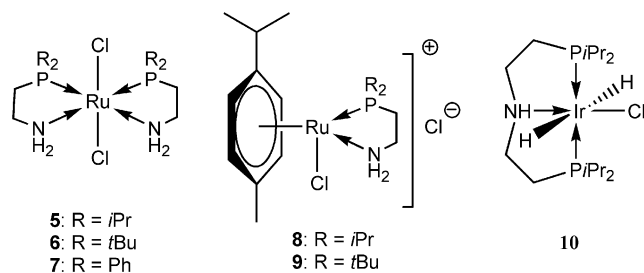
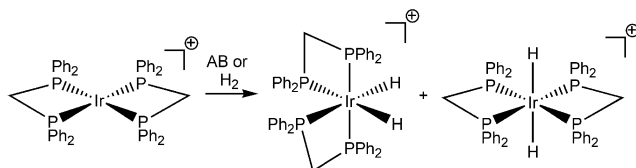


Figure 3. Ruthenium and iridium alcohol oxidation/reduction catalysts.<sup>[36]</sup>

A (POCOP)-based iridium hydride complex has been reported to produce pentamer from AB in nearly quantitative fashion.<sup>[22]</sup> Peruzzini et al. had recently been investigating the chemistry of  $[\text{Ir}(\text{dppm})_2]\text{OTf}$  [dppm = bis(diphenylphosphanyl)methane,  $\text{OTf} = (\text{CF}_3\text{O}_3\text{S})^-$ ], and based on the aforementioned results decided to test its reactivity with



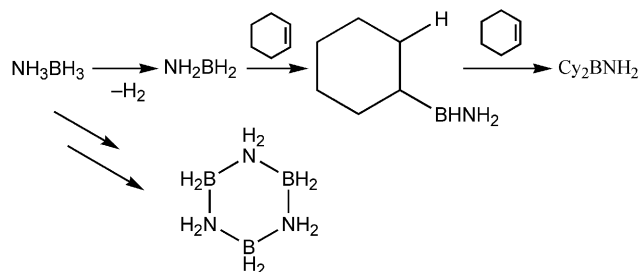
AB.<sup>[39]</sup> A 1:1 mixture of  $[\text{Ir}(\text{dppm})_2]\text{OTf}$  and AB in THF at  $-78^\circ\text{C}$  results in the formation of a brown precipitate and a mixture of the *cis*- and *trans*-isomers of  $[\text{Ir}(\text{dppm})_2\text{H}_2]^+$  which can also be obtained through the direct reaction of  $[\text{Ir}(\text{dppm})_2]\text{OTf}$  with  $\text{H}_2$  (Scheme 4). The same result is seen when up to three equivalents of AB are added. Using  $^{11}\text{B}$  NMR, there were no boron containing species observed in solution, indicating that all of the boron is “locked up” in the precipitate. While NMR, MS, and IR data could not elucidate the identity of the precipitate, it was found to be inconsistent with the pentameric product observed from  $(\text{POCOP})\text{IrH}_2$ .  $[\text{Ir}(\text{dppm})_2]\text{OTf}$  reacts with neither  $\text{NH}_3$  nor  $i\text{Pr}_2\text{NH}$ , but does react with  $\text{BH}_3\cdot\text{L}$  ( $\text{L} = \text{NH}_3, \text{THF}, \text{SMe}_2$ ) to form  $[\text{Ir}(\text{dppm})_2\text{H}_2]^+$  via  $[\text{Ir}(\text{dppm})_2\text{HX}]^+$  as confirmed by variable-temperature NMR experiments. The reaction with  $\text{B}_2\text{H}_6$  results in the direct formation of  $[\text{Ir}(\text{dppm})_2\text{H}_2]^+$ , even at low temperature. The identity of X could not be established with certainty due to the low concentration of  $[\text{Ir}(\text{dppm})_2\text{HX}]\text{OTf}$  relative to  $\text{BH}_3\cdot\text{L}$ . However, DFT calculations at the MPW1K11//6-31+g(d,p) level support a  $[\text{Ir}(\text{dppm})_2\text{H}(\text{BH}_2\text{NH}_3)]^+$  intermediate. No reaction was observed with  $\text{BH}_3\cdot\text{NHC}$ .<sup>[40]</sup> These binding experiments show that it is clear in this system that dehydrogenation is initiated by B–H bond cleavage. There is also work by Aldridge et al. on a bis(NHC)-iridium complex<sup>[41]</sup> that has the potential to demonstrate similar chemistry, but only a brief mention was made that excess AB could be used to generate a dihydride. In any case, the complex is unlikely to be a competitive AB dehydrogenation catalyst due to the reported 100 h half-life when dehydrogenating  $i\text{Pr}_2\text{NHBH}_3$  at  $50^\circ\text{C}$ .



Scheme 4. Hydrogenation of  $[\text{Ir}(\text{dppm})_2]\text{OTf}$ .<sup>[39]</sup>

Homogeneous catalysts are more amenable to facile study, but from an engineering point of view, a heterogeneous dehydrogenation catalyst is preferable as it would allow easy separation of the spent fuel. In this vein, Burrell and co-workers recently reported on the dehydrogenation of AB using platinum, palladium, and ruthenium supported on alumina, activated carbon, and alumina respectively.<sup>[42]</sup> All three materials induced the evolution of  $\text{H}_2$  from AB, but it was found that platinum yielded the greatest rate and extent of  $\text{H}_2$  release at 0.08 g/s of  $\text{H}_2$  per kilogram of AB over 15 minutes at  $70^\circ\text{C}$ , which constitutes 1.25 equivalents of  $\text{H}_2$ . Using  $^{11}\text{B}$  NMR, the reaction intermediates cyclodiborazane, cyclotriborazane, and borazine<sup>[43]</sup> were identified along with the polymerization product polyborazylene. The presence of the intermediate aminoborane (the significance of which will be discussed later) was also identified via its trapping with cyclohexene to form  $\text{C}_6\text{H}_{11}\text{BNH}_2$  (a methodology developed in this regard by Baker et al.<sup>[44]</sup>) (Scheme 5).

Catalytic activity was observed to decrease along with the formation of white precipitate, identified as polyborazylene, over several cycles. However, it was found that catalytic activity could be recovered through sonication and heating, indicating that the decrease in activity was due to physical blockage of the active sites and not chemical deactivation.

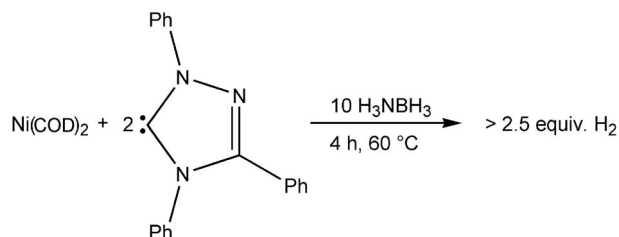


Scheme 5. Trapping of aminoborane by cyclohexene.<sup>[42,44]</sup>

### 3. Mechanisms of Dehydrogenation

#### 3.1. Experimental Observations of $\text{Ni}(\text{NHC})_2$

Baker's  $\text{Ni}(\text{NHC})_2$  complex (vide supra) was originally reported as a species generated in situ from  $\text{Ni}(\text{COD})_2$  and two equivalents of Enders' NHC (Scheme 6). Experiments with synthesizing analogous ruthenium and rhodium complexes showed that nickel had a higher rate of dehydrogenation (twice that of ruthenium and four times that of rhodium), and  $^{11}\text{B}\{^1\text{H}\}$  NMR analysis of the dehydrogenation products indicated the presence of  $(\text{HBNH})_n$ , a small amount of  $(\text{H}_2\text{BNH}_2)_n$ , and borazine with complete consumption of AB. Kinetic isotope effects were measured,  $\text{H}_3\text{NBD}_3$  (1.7),  $\text{D}_3\text{NBH}_3$  (2.3), and  $\text{D}_3\text{NBD}_3$  (3.0), showing that both N–H and B–H bond dissociations are involved in determining the reaction rate. From this data and the dehydrogenation of substituted amine boranes, it was proposed that the reaction is initiated by the oxidative addition of a B–H bond to the metal catalyst followed by  $\beta$ -H elimination at nitrogen to release  $\text{H}_2$  and  $\text{H}_2\text{NBH}_2$ .



Scheme 6. Dehydrogenation of AB by a Ni-carbene.<sup>[28]</sup>

#### 3.2. Calculations on $\text{Ni}(\text{NHC})_2$

In 2008, Hall and Yang reported DFT calculations (TPSS/cc-pVDZ) on the mechanism of release of the first equivalent of  $\text{H}_2$  from AB by  $\text{Ni}(\text{NHC})_2$  (Figure 4),<sup>[45]</sup> which was recently expanded to include work on the loss of

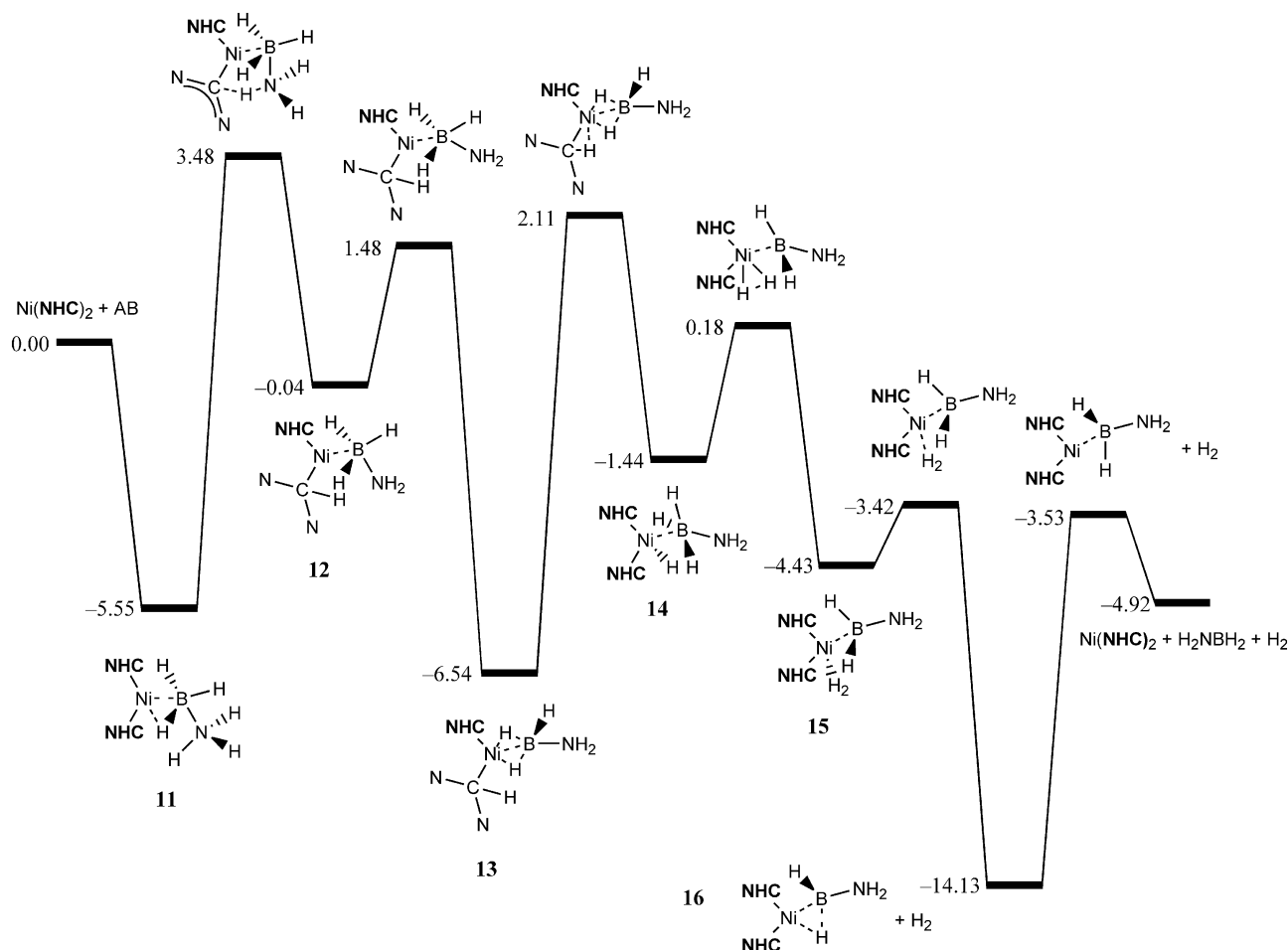


Figure 4. Calculated mechanism (TPSS/CC-PVDZ) for the loss of the first equivalent of H<sub>2</sub> from AB catalyzed by Ni(NHC)<sub>2</sub>. Energies are relative gas-phase enthalpies in kcal mol<sup>-1</sup>.<sup>[45]</sup>

the second equivalent (Figure 5).<sup>[46]</sup> The reaction between Ni(NHC)<sub>2</sub> and AB begins with coordination of nickel to AB via boron and a Ni–H–B bridge to form intermediate **11**. The reaction then proceeds further via proton transfer from the nitrogen center to a carbene to give the protonated carbene ligand **12**. Rotation about the Ni–B bond gives the more stable structure **13** containing two hydride bridges between nickel and boron. Nickel then activates the newly created C–H bond and the proton is transferred to nickel to provide **14**. H<sub>2</sub> formation occurs at nickel, giving **15**, followed by the release of H<sub>2</sub>, which results in **16**. Loss of aminoborane from **16** subsequently regenerates the original catalyst. Alternatively, **16** can react with free aminoborane to generate N<sub>2</sub>B<sub>2</sub>H<sub>6</sub> and H<sub>2</sub>. This begins with activation of the 3-center, 2-electron bond in **16** followed by transfer of a carbene ligand from nickel to boron resulting in **17**, which undergoes N–H activation to form dihydrogen complex **18**. Release of H<sub>2</sub> from **18** allows nickel to participate in B–C bond activation to retrieve its original carbene ligand and bind the remaining NHBH fragment in a side-on manner (see **20**). Free aminoborane can react with **20** to form **21** which undergoes rearrangement and release of N<sub>2</sub>B<sub>2</sub>H<sub>6</sub> to reform Ni(NHC)<sub>2</sub>.

### 3.3. Calculations on Ni(NHC) + NHC

Further complicating the picture, Musgrave et al.<sup>[47]</sup> also examined possible mechanistic pathways for the loss of the first equivalent of H<sub>2</sub> using DFT calculations (B3LYP, mixed basis set of 6-31++G\*\* on nickel, nickel hydrides, and AB and 6-31G\* on the NHC ligands) and found that it is likely that there are multiple active species (Scheme 7). AB initially adds to Ni(NHC)<sub>2</sub>, displacing one carbene ligand to form **23**. The free carbene reacts with another equivalent of AB to abstract H<sub>2</sub> and release aminoborane. While **23** and **24** were not found to competitively react with AB, upon elimination of H<sub>2</sub> they form **25** which does undergo displacement of aminoborane by AB. From these calculations, it appears that the active metal catalyst is carbene ligand based. In investigating the effect of free NHC using similar methods, it was found that it is likely not an innocent spectator in dehydrogenation (Scheme 8).<sup>[48]</sup> Free carbene can stoichiometrically react with AB, but on its own it does not react further with respect to dehydrogenation. NHC–(H)<sub>2</sub> can however undergo C–H activation in the presence of **25** to form insertion product **26** which itself can undergo a second C–H activation and subsequent elimi-

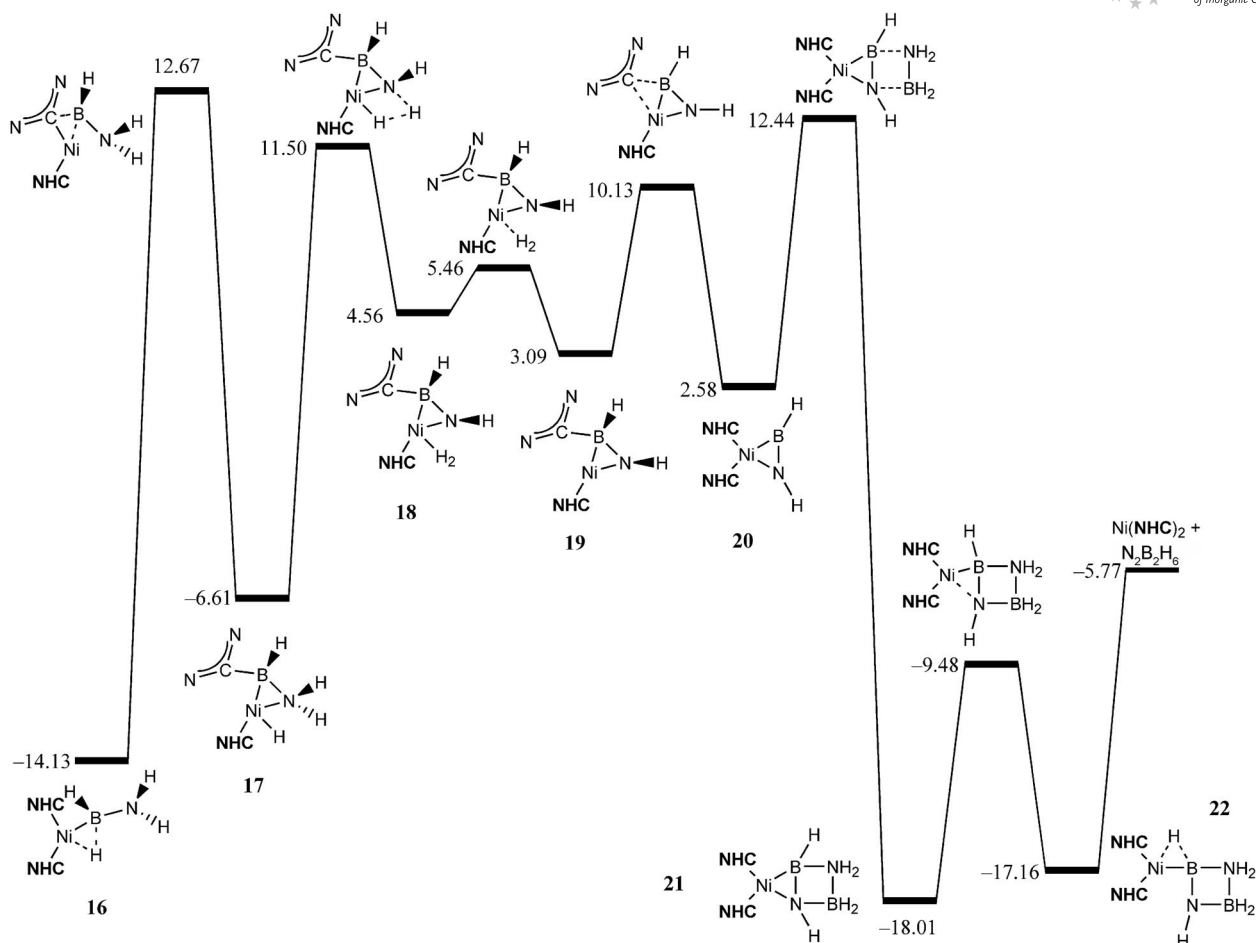
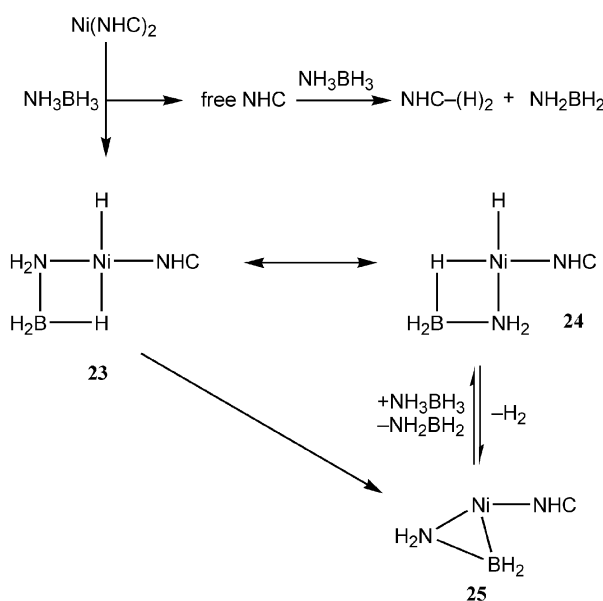


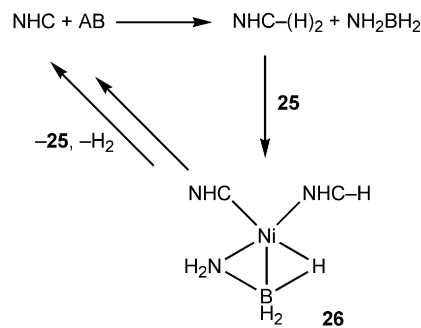
Figure 5. Calculated mechanism (TPSS/cc-PVDZ) for the loss of the second equivalent of  $\text{H}_2$  from AB catalyzed by  $\text{Ni}(\text{NHC})_2$ . Energies are relative gas-phase enthalpies in  $\text{kcal mol}^{-1}$ .<sup>[46]</sup>

nation of  $\text{H}_2$  to reform **25** and free carbene. These studies indicate that it is likely that there are multiple pathways for release of the first equivalent of  $\text{H}_2$  in the Ni-NHC system,

but that all involve the release of aminoborane. The release of the latter fragment appears to be a critical issue in determining the nature of the end product of dehydrogenation.



Scheme 7. AB dehydrogenation by monocarbene nickel.<sup>[47]</sup>



Scheme 8. Regeneration of free NHC.<sup>[48]</sup>

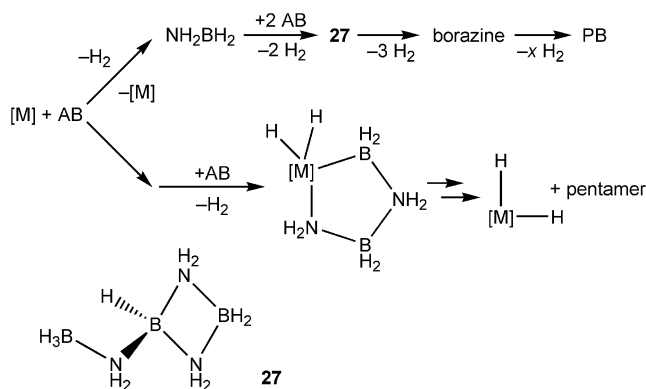
### 3.4. $(\text{NHBH})_n$ vs. $(\text{NH}_2\text{BH}_2)_n$

The ability to exercise control over the nature of the reaction product(s) (or spent fuel material) resulting from the dehydrogenation of AB is crucial in determining its potential utility as a fuel; the ability to influence the extent of dehydrogenation is important with respect to maximizing

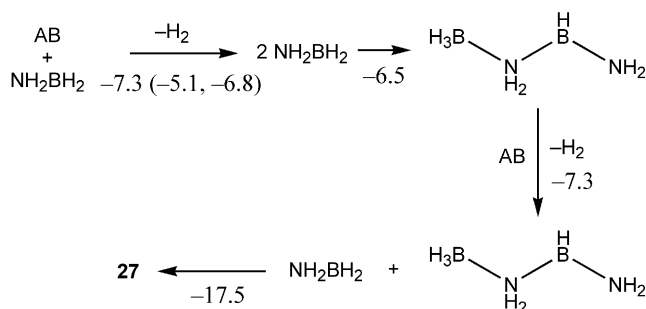
the gravimetric efficiency of AB as well as allowing for chemical regeneration of the spent fuel back into AB. Some dehydrogenation products are undesirable and must be avoided. Examples of this are: borazine, which is volatile and may poison the  $\text{H}_2$  stream for a fuel cell, and lead to inefficiency due to loss of mass, and pentamer, as it is insoluble and thus unsuited to a flow-type reactor.

Different catalysts yield different AB dehydrogenation products, and recent work by Baker, Dixon, and co-workers<sup>[44]</sup> has attempted to explain this by looking at (POCOP)IrH<sub>2</sub> which forms pentamer at 25 °C in diglyme and [Rh(1,5-COD)(μ-Cl)]<sub>2</sub> which forms PB/borazine under the same conditions. Trapping experiments with cyclohexene (Scheme 5) revealed that the formation of PB is preceded by the release of aminoborane into solution, while when pentamer is formed there is no evidence for free aminoborane in solution. These observations suggest divergent reaction pathways (Scheme 9) in which either the catalyst coordinates  $\text{H}_2$  or aminoborane, and this fact dictates the end-products and the ultimate extent of  $\text{H}_2$  release. Further experimental support for this hypothesis was seen in the identification by NMR and IR spectroscopic methods of intermediate **27** (Scheme 10), a precursor to borazine, following the dehydrogenation of AB by Ni(NHC)<sub>2</sub> at 25 °C. Thus, it can be seen that the key to producing more than one equivalent of  $\text{H}_2$  and a soluble dehydrogenated product is a catalyst that facilitates the production of free aminoborane. While free aminoborane is important to the extent of  $\text{H}_2$  release, it is not the only factor affecting the reaction. It was observed that even at 70 °C for 24 h in diglyme, solutions of **27** were stable. It is only when, in this case, rhodium catalyst was added that PB and borazine appeared. This indicates that metallic species play an undetermined role that is greater than just dehydrogenating AB to form aminoborane. It is unclear what, if any, role CTB plays in the formation of borazine as it is not mentioned as being observable. A previous study<sup>[43]</sup> on the thermolysis of AB in glyme demonstrated the appearance of borazine before significant quantities of CTB could be detected. Therefore, the order in which borazine and CTB formed could not be determined. Other work has shown that there is little to no conversion of CTB to borazine at temperatures below ca. 130 °C.<sup>[49]</sup> However, the presence of a metal complex may change the mechanistic pathway(s) of borazine formation from that of pure thermolysis.

The separation of catalysts into two neatly separate categories of “releases aminoborane” and “does not release aminoborane” is attractive in its simplicity, but observed reactivity indicates the mechanism(s) are more complicated. At 25 °C, addition of cyclohexene to the Ni(NHC)<sub>2</sub>-catalyzed dehydrogenation of AB does not result in the formation of  $\text{C}_2\text{B}_2\text{NH}_2$ ; only PB and **27** are observed. It is not until the reaction is heated to 60 °C that  $\text{C}_2\text{B}_2\text{NH}_2$  is formed, but contrary to [Rh(COD)Cl]<sub>2</sub> and Ir(POCOP)H<sub>2</sub> under the same conditions, PB is also observed. Clearly there is an alternative pathway in the presence of Ni(NHC)<sub>2</sub>, and it may involve the free carbene ligand, but experimental insight into this is unavailable at this juncture.



Scheme 9. AB dehydrogenation pathways.<sup>[44]</sup>



Scheme 10. Aminoborane reactivity with AB (G3MP2 enthalpies at 298 K in kcal mol<sup>-1</sup>, the numbers in parentheses indicate 298 K and 0 K CCSD(T)/CBS values<sup>[50]</sup>). Compound **27** is the kinetically favored isomer.<sup>[44]</sup>

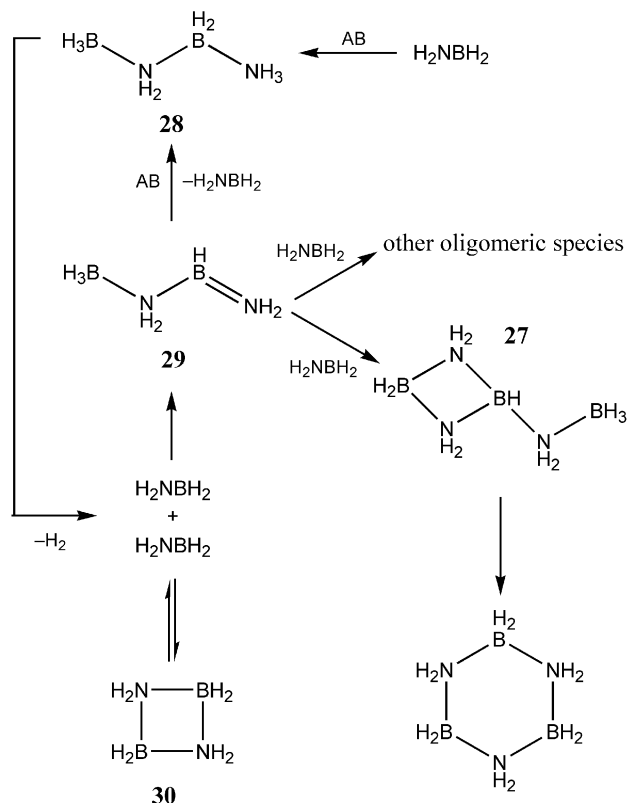
### 3.5. The Effect of Free $\text{NH}_2\text{BH}_2$

With the observation that catalysts that release aminoborane yield a more desirable PB dehydrogenation product, it is important to understand the detailed role that free aminoborane plays. While it is nontrivial to study the reactivity of this fragment experimentally due to its transient nature, it has been studied by Zimmerman et al. computationally using ab initio CCSD(T) simulations [CCSD(T)//MP2/cc-pVTZ, Scheme 11].<sup>[51]</sup> Aminoborane can react with AB to form linear dimer **28**. Under the driving force of loss of  $\text{H}_2$ , **28** decomposes to two equivalents of aminoborane, which can equilibrate with cyclic dimer **30** or convert into linear dimer **29**. Dimer **29** can then further react with aminoborane to form oligomeric species, one of which is **27** [which has been observed experimentally (vide supra)]. Compound **27** can then undergo rearrangement to form CTB. In this manner, “free” aminoborane can be autocatalytic for the formation of CTB which is consistent with the hypothesis that catalysts that retain aminoborane generate pentamer through ring expansion at the metal center (Scheme 9). Alternatively, a previous DFT [B3LYP/6-311+G(2d,p)//B3LYP/6-31G(d)] study by Nutt and McKee<sup>[52]</sup> suggests that CTB is unlikely to be an intermediate in the formation of borazine from three aminoborane fragments due to larger free-energy barriers than other pathways, and calculations by Dixon et al.<sup>[44]</sup> (Scheme 10) also argue for an alternative reaction mechanism. However,



all studies are consistent with “free” aminoborane being a reactive fragment that is capable of inducing further dehydrogenation (Figure 6, Figure 7). A consequence of the reactivity of aminoborane towards AB is that it greatly com-

plicates the mechanistic study of catalysts that produce PB. In the easiest possible case, the metal catalyst and released aminoborane would simply work in tandem. More likely though is that there will be competitive reactions with either metal-mediated enhancement or retardation and varying degrees of metal interaction with the oligomer intermediates.



Scheme 11. Calculated reaction pathways of aminoborane [CCSD(T)//MP2/cc-pVTZ].<sup>[51]</sup>

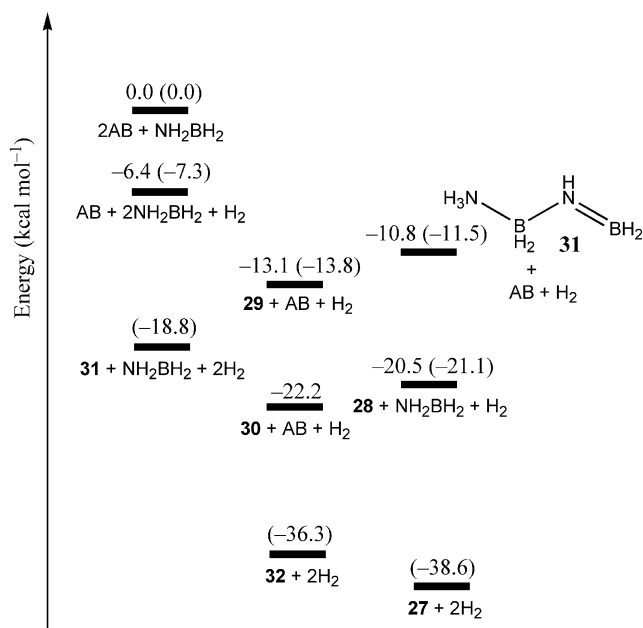


Figure 6.  $2\text{AB} + \text{NH}_2\text{BH}_2$  0 K (298 K) enthalpies ( $\text{kcal mol}^{-1}$ ) using CCSD(T)//MP2/cc-pVTZ<sup>[51]</sup> (G3MP2).<sup>[44]</sup>

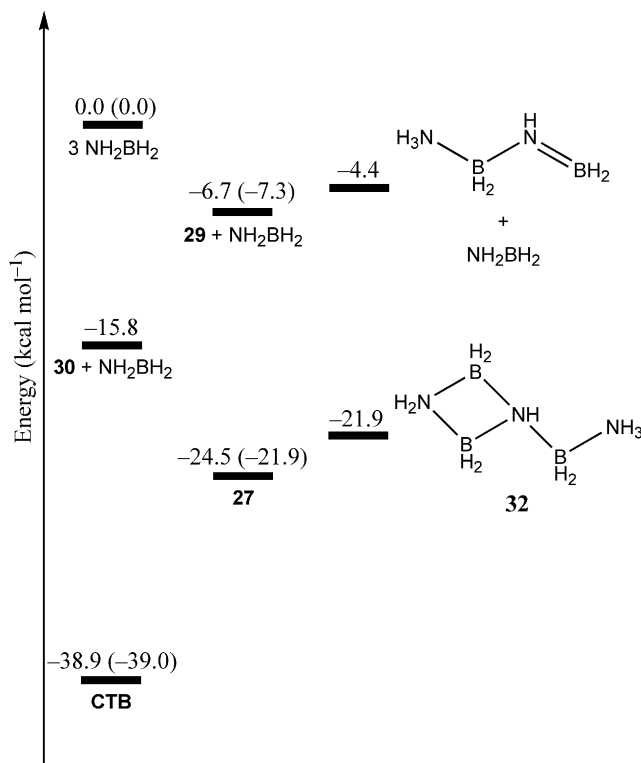


Figure 7.  $3\text{NH}_2\text{BH}_2$  0 K (298 K) enthalpies ( $\text{kcal mol}^{-1}$ ) using CCSD(T)//MP2/cc-pVTZ<sup>[51]</sup> (G3MP2).<sup>[44]</sup> The CCSD(T)/CBS value for the formation of CTB from  $3\text{NH}_2\text{BH}_2$  is  $-39.7 \text{ kcal mol}^{-1}$ .<sup>[50]</sup>

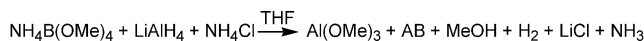
#### 4. Regeneration

A key component of a practical scheme for the use of  $\text{H}_2$  as a transportation fuel is the ability to regenerate the hydrogen carrier in a cost efficient and sustainable manner. More so than with the release of  $\text{H}_2$  from a carrier, the challenge of regeneration is intimately entwined with the engineering costs of large scale industrial processes. Even though it may be possible to regenerate a particular form of spent fuel with good yields and rates, the reagents used can be too expensive, overly hazardous, or too difficult to utilize on the scale required for mass fuel production. The potential costs of regeneration have previously prompted the DOE to make “no go” decisions on materials such as  $\text{NaBH}_4$ . Therefore for AB to remain a viable candidate as a  $\text{H}_2$  carrier, the issue of regeneration must be addressed, and it may impose restrictions on what sort of dehydrogenation schemes are reasonable. Due to the thermodynamics of AB dehydrogenation,<sup>[53]</sup> off-board regeneration of the

spent fuel is likely to be required, where off-board regeneration is removal of the spent fuel from a vehicle and regeneration occurring at a processing plant. It is also evident that ceramic BN (fully dehydrogenated AB) is energetically undesirable as it represents a thermodynamic sink. This limits the usable H<sub>2</sub> density of AB, but the 18 wt.-% of H<sub>2</sub> release reported by Baker demonstrates that metal-catalyzed dehydrogenation is capable of H<sub>2</sub> release well above the DOE target of 7.5 wt.-% while still generating “spent fuel” that is energetically feasible to regenerate.

#### 4.1. Solvolysis

Approaches to AB dehydrogenation using solvolysis involve the formation of B–O bonds which are thermodynamically much more stable than the oligomeric B–N containing products. This extra heat loss not only increases the difficulty in regeneration and makes for a system thermodynamically further away from on-board regeneration ( $\Delta G \approx 0$ ), but also lowers energy efficiency. Nonetheless, a scheme for the regeneration of AB from methanolysis (Scheme 12) has been published<sup>[54]</sup> and previously discussed<sup>[11]</sup> that utilizes the reduction of NH<sub>4</sub>B(OMe)<sub>4</sub> by LiAlH<sub>4</sub>. However, this process results in the loss of H<sub>2</sub> and NH<sub>3</sub> which must be trapped and recycled and the formation of Al(OMe)<sub>3</sub> which must be converted back to LiAlH<sub>4</sub>.

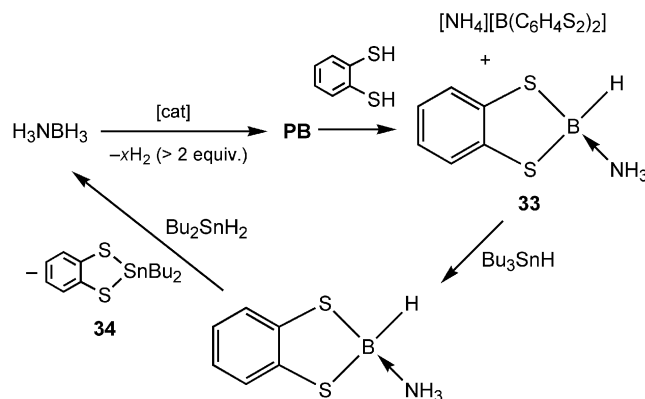


Scheme 12. Regeneration of AB from NH<sub>4</sub>B(OMe)<sub>4</sub>.<sup>[54]</sup>

#### 4.2. Polyborazylene

Both metal-catalyzed dehydrogenation and thermolysis (at temperatures below ca. 500 °C, above which, evidence for boron nitride is seen<sup>[55]</sup>) lead to products of the type (H<sub>2</sub>NBH<sub>2</sub>)<sub>n</sub> and/or (HNBH)<sub>n</sub>. Similar strategies for regenerating AB from mixtures of these products have been proposed by Sneddon<sup>[56,57]</sup> and Mertens<sup>[58]</sup> that do not depend on the nature of (H<sub>2</sub>NBH<sub>2</sub>)<sub>n</sub> or (HNBH)<sub>n</sub> by using an acid (HX) to form B–X bonds and then conversion of those B–

X bonds into B–H bonds. The current progress and issues with this approach have largely been previously summarized.<sup>[11]</sup> A new approach to the regeneration problem (Scheme 13) involves restricting the dehydrogenation product to something that is relatively well-defined so that the chemistry can be more finely tuned.<sup>[59]</sup> PB is an obvious choice for this as it requires that more than two equivalents of H<sub>2</sub> be released, thus maximizing H<sub>2</sub> yield. PB is also soluble in common organic solvents so it is potentially compatible with a flow-type reactor. DFT calculations (gas-phase: B3LYP/DZVP2, cc-pVDZ-PP for tin) (Tables 1 and 2) on the reaction of thiophenol with borazine (a computational surrogate for PB) predicted endothermic enthalpies in the condensed and gas phases, but that the reaction between chelating 1,2-benzenedithiol and borazine would be thermodynamically favorable. The latter prediction was borne out by performing the digestion of PB with 1,2-benzenedithiol in refluxing THF to give a mixture of **33** (<sup>11</sup>B NMR,  $\delta = -5.6$  ppm) and [NH<sub>4</sub>][B(C<sub>6</sub>H<sub>4</sub>S<sub>2</sub>)<sub>2</sub>] (<sup>11</sup>B NMR,  $\delta = 10.5$  ppm).



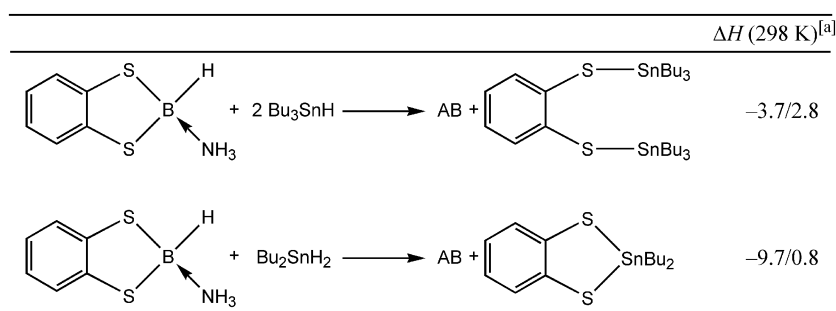
Scheme 13. Regeneration of AB from polyborazylene.<sup>[59]</sup>

An initially attractive reducing agent for **33** was Bu<sub>3</sub>SnH as it is commercially available and a literature report on the thermodynamics of the reaction between Bu<sub>3</sub>SnH and CO<sub>2</sub><sup>[60]</sup> suggests a potential recycling pathway in the form of decarboxylation of tin formate (Figure 8). While Bu<sub>3</sub>SnH did not generate AB from **33**, it did convert [NH<sub>4</sub>]-

Table 1. Calculated digestion enthalpies of borazine (gas-phase: B3LYP/DZVP2, cc-pVDZ-PP for tin).<sup>[59]</sup>

			$\Delta H$ (298 K) <sup>[a]</sup>
		42.2/25.1	
		-20.4/0.5	

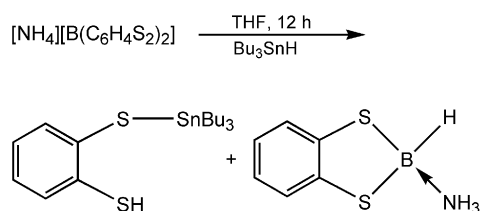
[a] Condensed-phase/gas-phase (kcal mol<sup>-1</sup>).

Table 2. Calculated enthalpies of reduction of **33** (gas-phase: B3LYP/DZVP2, cc-pVDZ-PP for tin).<sup>[59]</sup>[a] Condensed-phase/gas-phase (kcal mol<sup>-1</sup>).

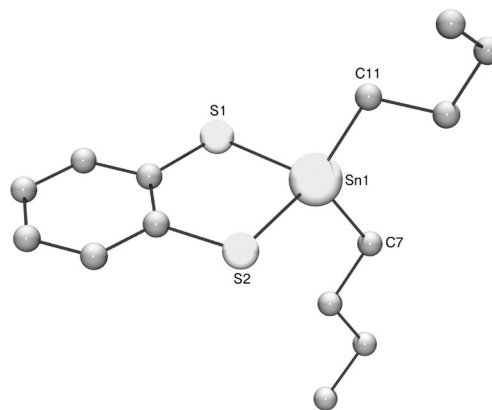
[B(C<sub>6</sub>H<sub>4</sub>S<sub>2</sub>)<sub>2</sub>] to **33** quantitatively (Scheme 14), providing a two-step conversion to a single B–H-containing species from PB. Further attempts to reduce **33** with other reducing agents resulted in no reaction or over-reduction to borohydride. Continued screening of potential reducing agents using DFT calculations suggested the use of Bu<sub>2</sub>SnH<sub>2</sub> to overcome the chelate effect of the 1,2-benzenedithiolate ligand. Experimental results confirmed this prediction when the addition of Bu<sub>2</sub>SnH<sub>2</sub> to **33** resulted in the formation of **34** (Figure 9, Table 3) and AB. This successfully demonstrated a fuel regeneration cycle, which is summarized in Scheme 13. An isolated yield of AB from PB of 67% was obtained. More recently, DuBois et al. reported the formation of triethylamine borane with ca. 90% conversion from B(SPh)<sub>3</sub> in the presence of triethylamine using the rhodium hydride HRh(dmpe)<sub>2</sub> [dmpe = 1,2-bis(diethylphosphanyl)ethane)].<sup>[61]</sup> However, reactions with **33** did not result in conversion from B–S to B–H bonds.



$$\begin{aligned} \Delta H &= -18.3 \pm 0.2 \text{ kcal mol}^{-1} \\ \Delta S &= -20.2 \pm 0.2 \text{ cal mol}^{-1} \text{ K}^{-1} \end{aligned}$$

Figure 8. Bu<sub>3</sub>SnH/Bu<sub>3</sub>SnO<sub>2</sub>CH equilibrium.<sup>[60]</sup>Scheme 14. Reduction of [NH<sub>4</sub>][B(C<sub>6</sub>H<sub>4</sub>S<sub>2</sub>)<sub>2</sub>] with Bu<sub>3</sub>SnH.<sup>[59]</sup>

Using the approximation of efficiency given by Equation (1), this process is estimated to be 65% efficient with regard to the energy input required which compares quite favorably with the estimated 46% efficiency in recovering AB from NH<sub>4</sub>B(OMe)<sub>4</sub>. In the analysis of an optimized version of this regeneration Scheme, it has been calculated that such a process could be up to 80% thermodynamically efficient.<sup>[62]</sup> Analysis also indicates that the generation of formic acid and the cost of mass transport of tin are a signifi-

Figure 9. Ball-and-stick representation of the crystal structure of **34**. Unlabeled atoms are carbon, hydrogen atoms omitted for clarity.<sup>[59]</sup>Table 3. Bond lengths and angles of **34**.<sup>[59]</sup>

Length [Å]		Angle [°]	
Sn1–S1	2.4183 (0.0007)	S1–Sn1–S2	90.46 (0.02)
Sn1–S2	2.4217 (0.0007)	C11–Sn1–C7	121.05 (0.09)
Sn1–C7	2.1338 (0.0024)	S1–Sn1–C11	111.01 (0.06)
Sn1–C11	2.1297 (0.0022)	S1–Sn1–C7	110.37 (0.07)
		S2–Sn1–C11	109.93 (0.07)
		S2–Sn1–C7	109.80 (0.07)

cant portion of the fuel regeneration cost, leaving room for improvement for a process that is estimated to have a cost equivalent of ca. \$7–8 per kg of H<sub>2</sub>.<sup>[63]</sup>

$$\% \text{ efficiency} = \frac{(\text{equiv. H}_2 \text{ stored})(57.8)}{(\text{equiv. H}_2 \text{ used})(57.8) + \sum (\Delta H_{\text{endo}}) - (\% \text{ heat recovered}) \sum (-\Delta H_{\text{exo}})}$$

Estimated energy efficiency of a H<sub>2</sub> regeneration scheme.<sup>[59]</sup> (1)

Work is currently underway within the DOE Chemical Hydrogen Storage Center of Excellence to improve the overall efficiencies of regeneration chemistries for potential scale-up.

## 5. The Future of Metal-Catalyzed Dehydrogenation of AB

While much progress has been made in understanding the metal-catalyzed dehydrogenation of AB and the issues that affect the resultant end product(s), there are still areas that require further investigation. On the catalyst development front, there is a gap between dehydrogenation extent and rate where the catalysts that show the greatest extent are typically the slowest. Most catalysts are still based on precious metals, which is not feasible from both cost and material availability perspectives on a global scale. Thus, more effort needs to be put forth toward developing base metal catalysts which are less expensive and more abundant. A flow reactor will also require a heterogeneous catalyst that is tethered to a support or immobilized in a matrix in order to maintain separation of the fuel and the catalyst. Some work has been done with supported metal sites, but the majority of known dehydrogenation catalysts are solution-based. This is not to imply that solution chemistry should be abandoned, as soluble complexes are more easily characterized and studied, but rather that strategies for immobilization should be kept in mind and pursued during catalyst development.

As AB is a solid at ambient temperatures, there needs to be some effort focused on moving to liquid versions for practical usage. While the details of the approaches to this problem are beyond the scope of this review, it should be noted that use of a solvent can seriously impact the gravimetric H<sub>2</sub> capacity of the fuel and that using an appropriate mixture of AB and substituted aminoborane(s)<sup>[64]</sup> necessitates that any catalyst still behave in a well-defined manner and not release other gaseous products that may poison a fuel cell. Issues with regeneration of these systems would also have to be addressed. Due to the exothermicity of the dehydrogenation of AB, on-board regeneration of spent fuel is unlikely, though other B–N derivatives are also being explored in order to bring the release of H<sub>2</sub> as close to thermoneutral as possible.

## 6. Conclusions

The 19.6 wt.-% H<sub>2</sub> in AB has made it an attractive molecule for chemical hydrogen storage, and it is made more so by its stability and nontoxicity. The challenges of its use include controlled dehydrogenation, it being a solid at room temperature, and regeneration (refueling). Within the scope of this review, good progress has been made in understanding the factors that control the dehydrogenation products and the extent of H<sub>2</sub> release by using both experimental observations and theoretical calculations. An important aspect of maximizing the extent of H<sub>2</sub> release is that a metal catalyst needs to promote release of aminoborane rather than generate a pentamer through ring expansion on the catalyst metal center. Aminoborane can also play a key role as it oligomerizes autocatalytically. More work remains to be done on determining what the factors are that dictate

how a given catalyst reacts with AB and on translating the chemistry observed in solution to a supported heterogeneous framework.

## Acknowledgments

This work was funded by the U.S. Department of Energy, Office of Energy Efficiency and Renewable Energy. We would like to thank Drs. Kevin Ott and Andrew Sutton for their suggestions and comments on improving this manuscript.

- [1] L. Schlapbach, A. Züttel, *Nature* **2001**, 414, 353–358.
- [2] S. Satyapal, J. Petrovic, C. Read, G. Thomas, G. Ordaz, *Catal. Today* **2007**, 120, 246–256.
- [3] *Technical System Targets: On-Board Hydrogen Storage for Light-Duty Vehicles* ([http://www1.eere.energy.gov/hydrogen-and-fuelcells/storage/pdfs/targets\\_onboard\\_hydro\\_storage.pdf](http://www1.eere.energy.gov/hydrogen-and-fuelcells/storage/pdfs/targets_onboard_hydro_storage.pdf)).
- [4] T. B. Marder, *Angew. Chem. Int. Ed.* **2007**, 46, 8116–8118.
- [5] F. H. Stephens, V. Pons, R. T. Baker, *Dalton Trans.* **2007**, 2613–2626.
- [6] A. Klerke, C. H. Christensen, J. K. Nørskov, T. Vegge, *J. Mater. Chem.* **2008**, 18, 2304–2310.
- [7] P. Wang, X.-d. Kang, *Dalton Trans.* **2008**, 5400–5413.
- [8] B. Peng, J. Chen, *Energy Environ. Sci.* **2008**, 1, 479–483.
- [9] P. Chen, M. Zhu, *Mater. Today* **2008**, 11, 36–43.
- [10] L. J. Murray, M. Dinca, J. R. Long, *Chem. Soc. Rev.* **2009**, 38, 1294–1314.
- [11] C. W. Hamilton, R. T. Baker, A. Staubitz, I. Manners, *Chem. Soc. Rev.* **2009**, 38, 279–293.
- [12] U. Eberle, M. Felderhoff, F. Schüth, *Angew. Chem. Int. Ed.* **2009**, 48, 6608–6630.
- [13] D. J. Grant, D. A. Dixon, *J. Phys. Chem. A* **2006**, 110, 12955–12962.
- [14] K. W. Boeddeker, S. G. Shore, R. K. Bunting, *J. Am. Chem. Soc.* **1966**, 88, 4396–4401.
- [15] C. T. Kwon, H. A. McGee Jr., *Inorg. Chem.* **1970**, 9, 2458–2461.
- [16] Y. D. Blum, R. M. Laine, *US Pat.*, 4 801 439, **1989**.
- [17] I. G. Green, K. M. Johnson, B. P. Roberts, *J. Chem. Soc. Perk. Trans. 2* **1989**, 1963–1972.
- [18] C. A. Jaska, K. Temple, A. J. Lough, I. Manners, *Chem. Commun.* **2001**, 962–963.
- [19] C. A. Jaska, K. Temple, A. J. Lough, I. Manners, *J. Am. Chem. Soc.* **2003**, 125, 9424–9434.
- [20] Y. Chen, J. L. Fulton, J. C. Linehan, T. Autrey, *J. Am. Chem. Soc.* **2005**, 127, 3254–3255.
- [21] J. L. Fulton, J. C. Linehan, T. Autrey, M. Balasubramanian, Y. Chen, N. K. Szymczak, *J. Am. Chem. Soc.* **2007**, 129, 11936–11949.
- [22] M. C. Denney, V. Pons, T. J. Hebden, D. M. Heinekey, K. I. Goldberg, *J. Am. Chem. Soc.* **2006**, 128, 12048–12049.
- [23] I. Goettker-Schnetmann, P. S. White, M. Brookhart, *Organometallics* **2004**, 23, 1766–1776.
- [24] A. Paul, C. B. Musgrave, *Angew. Chem. Int. Ed.* **2007**, 46, 8153–8156.
- [25] T. J. Clark, C. A. Russell, I. Manners, *J. Am. Chem. Soc.* **2006**, 128, 9582–9583.
- [26] D. Pun, E. Lobkovsky, P. J. Chirik, *Chem. Commun.* **2007**, 3297–3299.
- [27] T. D. Forster, H. M. Tuononen, M. Parvez, R. Roesler, *J. Am. Chem. Soc.* **2009**, 131, 6689–6691.
- [28] R. J. Keaton, J. M. Blacquiere, R. T. Baker, *J. Am. Chem. Soc.* **2007**, 129, 1844–1845.
- [29] D. Enders, K. Breuer, G. Raabe, J. Runsink, J. H. Teles, J.-P. Melder, K. Ebel, S. Brode, *Angew. Chem. Int. Ed. Engl.* **1995**, 34, 1021–1023.
- [30] M. E. Sloan, T. J. Clark, I. Manners, *Inorg. Chem.* **2009**, 48, 2429–2435.



- [31] P. Rigo, M. Bressan, *Inorg. Chem.* **1976**, *15*, 220–223.
- [32] M. KäB, A. Friedrich, M. Drees, S. Schneider, *Angew. Chem. Int. Ed.* **2009**, *48*, 905–907.
- [33] R. Noyori, T. Okhuma, *Angew. Chem. Int. Ed.* **2001**, *40*, 40–73.
- [34] S. E. Clapham, A. Hadzovic, R. H. Morris, *Coord. Chem. Rev.* **2004**, *248*, 2201–2237.
- [35] K. Muniz, *Angew. Chem. Int. Ed.* **2005**, *44*, 6622–6627.
- [36] N. Blaquiere, S. Diallo-Garcia, S. I. Gorelsky, D. A. Black, K. Fagnou, *J. Am. Chem. Soc.* **2008**, *130*, 14034–14035.
- [37] M. T. Nguyen, V. S. Nguyen, M. H. Matus, G. Gopakumar, D. A. Dixon, *J. Phys. Chem. A* **2007**, *111*, 679–690.
- [38] A. Staubitz, A. P. Soto, I. Manners, *Angew. Chem. Int. Ed.* **2008**, *47*, 6212–6215.
- [39] A. Rossin, M. Caporali, L. Gonsalvi, A. Guerri, A. Lledós, M. Peruzzini, F. Zanobini, *Eur. J. Inorg. Chem.* **2009**, 3055–3059.
- [40] Y. Wang, B. Quillian, P. Wei, C. S. Wannere, Y. Xie, R. B. King, H. F. Schaefer III, P. v. R. Schleyer, G. H. Robinson, *J. Am. Chem. Soc.* **2007**, *129*, 12412–12413.
- [41] C. Y. Tang, W. Smith, D. Vidovic, A. L. Thompson, A. B. Chaplin, S. Aldridge, *Organometallics* **2009**, *28*, 3059–3066.
- [42] R. P. Shrestha, H. V. K. Diyabalanage, T. A. Semelsberger, K. C. Ott, A. K. Burrell, *Int. J. Hydrogen Energy* **2009**, *34*, 2616–2621.
- [43] W. J. Shaw, J. C. Linehan, N. K. Szymczak, D. J. Heldebrant, C. Yonker, D. M. Camaioni, R. T. Baker, T. Autrey, *Angew. Chem. Int. Ed.* **2008**, *47*, 7493–7496.
- [44] V. Pons, R. T. Baker, N. K. Szymczak, D. J. Heldebrant, J. C. Linehan, M. H. Matus, D. J. Grant, D. A. Dixon, *Chem. Commun.* **2008**, 6597–6599.
- [45] X. Yang, M. B. Hall, *J. Am. Chem. Soc.* **2008**, *130*, 1798–1799.
- [46] X. Yang, M. B. Hall, *J. Organomet. Chem.* **2009**, *694*, 2831–2838.
- [47] P. M. Zimmerman, A. Paul, C. B. Musgrave, *Inorg. Chem.* **2009**, *48*, 5418–5433.
- [48] P. M. Zimmerman, A. Paul, Z. Zhang, C. B. Musgrave, *Angew. Chem. Int. Ed.* **2009**, *48*, 2201–2205.
- [49] R. Schellenberg, J. Kriehme, G. Wolf, *Thermochim. Acta* **2007**, *457*, 103–108.
- [50] M. H. Matus, K. D. Anderson, D. M. Camaioni, S. T. Autrey, D. A. Dixon, *J. Phys. Chem. A* **2007**, *111*, 4411–4421.
- [51] P. M. Zimmerman, A. Paul, Z. Zhang, C. B. Musgrave, *Inorg. Chem.* **2009**, *48*, 1069–1081.
- [52] W. R. Nutt, M. L. McKee, *Inorg. Chem.* **2007**, *46*, 7633–7645.
- [53] C. R. Miranda, G. Ceder, *J. Chem. Phys.* **2007**, *126*, 184703/1–11.
- [54] P. V. Ramachandran, P. D. Gagare, *Inorg. Chem.* **2007**, *46*, 7810–7817.
- [55] M. G. Hu, R. A. Geanangel, W. W. Wendlandt, *Thermochim. Acta* **1978**, *23*, 249–255.
- [56] L. G. Sneddon, *Amineborane Hydrogen Storage – New Methods for Promoting Amineborane Dehydrogenation/Regeneration Reactions*, DoE Hydrogen Annual Progress Report, **2007** ([http://www.hydrogen.energy.gov/pdfs/progress07/iv\\_b\\_5e\\_sneddon.pdf](http://www.hydrogen.energy.gov/pdfs/progress07/iv_b_5e_sneddon.pdf)).
- [57] L. G. Sneddon, *Amineborane based Chemical Hydrogen Storage, DoE Hydrogen Annual Merit Review*, **2007** ([http://www.hydrogen.energy.gov/pdfs/review07/st\\_27\\_sneddon.pdf](http://www.hydrogen.energy.gov/pdfs/review07/st_27_sneddon.pdf)).
- [58] S. Hausdorf, F. Baitalow, G. Wolf, F. O. R. L. Mertens, *Int. J. Hydrogen Energy* **2008**, *33*, 608–614.
- [59] B. L. Davis, D. A. Dixon, E. B. Garner, J. C. Gordon, M. H. Matus, B. Scott, F. H. Stephens, *Angew. Chem. Int. Ed.* **2009**, *48*, 6812–6816.
- [60] R. J. Klingler, I. Bloom, J. W. Rathke, *Organometallics* **1985**, *4*, 1893–1894.
- [61] M. T. Mock, R. G. Potter, D. M. Camaioni, J. Li, W. G. Dougherty, W. S. Kassel, B. Twamley, D. L. DuBois, *J. Am. Chem. Soc.* **2009**, *131*, 14454–14465.
- [62] K. C. Ott, R. T. Baker, A. K. Burrell, B. L. Davis, H. V. Diyabalanage, J. C. Gordon, C. W. Hamilton, N. Henson, M. Inbody, K. D. John, T. A. Semelsberger, R. Shrestha, F. H. Stephens, *Chemical Hydrogen Storage R&D at Los Alamos National Laboratory, DOE Hydrogen Annual Progress Report*, **2008** ([http://hydrogen.energy.gov/pdfs/progress08/iv\\_b\\_1f\\_ott.pdf](http://hydrogen.energy.gov/pdfs/progress08/iv_b_1f_ott.pdf)).
- [63] K. C. Ott, *Overview - DOE Chemical Hydrogen Storage Center of Excellence, DOE Hydrogen Annual Review*, **2009** ([http://www.hydrogen.energy.gov/pdfs/review09/st\\_15\\_ott.pdf](http://www.hydrogen.energy.gov/pdfs/review09/st_15_ott.pdf)).
- [64] D. J. Grant, M. H. Matus, K. D. Anderson, D. M. Camaioni, S. R. Neufeldt, C. F. Lane, D. A. Dixon, *J. Phys. Chem. A* **2009**, *113*, 6121–6132.

Received: September 17, 2009

Published Online: December 22, 2009